

This ESI for *J. Mater. Chem. A*, 2020, DOI: 10.1039/C9TA10797E, originally published on 30th March 2020, was updated with the corrected Table S3 on 18th May 2020. Please see the accompanying Correction for further details (DOI: 10.1039/D0TA90096F).

Supporting Information for

Iron-based clusters embedded in nitrogen doped activated carbon catalysts with superior cathodic activity in microbial fuel cells

Xiaoyuan Zhang ^{a,*}, Xingguo Guo ^a, Qiuying Wang ^a, Rufan Zhang ^b, Ting Xu^a, Peng Liang ^a and Xia Huang ^a

^a State Key Joint Laboratory of Environment Simulation and Pollution Control, School of Environment, Tsinghua University, Beijing 100084, China

^b Department of Chemical Engineering, Tsinghua University, Beijing 100084, China

* Corresponding Author: E-mail: zhangxiaoyuan@tsinghua.edu.cn

Experimental Section

1. Synthesis of NAC and Fe-Clusters/NAC catalysts.

NAC and Fe-Clusters/NAC catalysts were prepared via a one-step ball milling method using a planetary ball mill machine (QM-3SP2, Nanjing University Instruments Plant). For NAC, 2 mL pyrrole (Sigma-Aldrich, 98%) was mixed with 1 g AC (Norit SX ultra cat, Norit Americas Inc. USA) as a mixture, and for Fe-Clusters/NAC, additional 0.5 g Fe₂O₃ (CAS: 1309-37-1, Aladdin, 99.5%) was added into that mixture. All the chemicals used in this work were analytical grade and used without further purification. For the ball milling

process, the ball and chemicals were in the weight ratio of 20:1, and the machine firstly worked at 450 rpm for 0.5 h, then 650 rpm for 3.5 h. Afterwards, the ball milled mixture was filtered using a 0.22 μm membrane, rinsed by deionized water, and dried at 80 $^{\circ}\text{C}$ for 6 h. Finally, in N_2 atmosphere, all the materials above were heated at 900 $^{\circ}\text{C}$ for 30 min (heating rate 6 $^{\circ}\text{C min}^{-1}$) via a tubular furnace and cooled to room temperature naturally to obtain the desired catalysts.

2. Preparation of air-cathodes

Air-cathodes (projected area 7 cm^2) in this work were similar to the reported ones ¹. To fabricate the diffusion layer, a uniform mixture consisting of 212 mg carbon black (Cabot, XC-72R) and 705.5 mg polytetrafluoroethylene (PTFE, 60% wt.) was rolled onto a stainless steel mesh (50 \times 50, type 304, McMasterCarr, USA), pressed under 4.5 MPa for 10 min, and then sintered at 340 $^{\circ}\text{C}$ for 20 min. As for the catalysts layer, a smooth paste with 20 mg catalyst, 80 mg AC and 40 μL PTFE was also rolled onto a stainless steel mesh. Then, to form an air-cathode, these two layers were pressed together (keeping the catalysts in the middle of two stainless steel meshes) under a pressure of 4.5 MPa for 20 min and heated at 80 $^{\circ}\text{C}$ for 10 min. In addition, AC and Pt/C (10% HPT010, HeSen, Shanghai, China) were also applied in air-cathodes as benchmarks.

3. Material characteristics

A scanning electron microscopy (SEM; MERLIN VP Compact; 20 kV) was employed to study the morphologies of catalysts. All the catalysts were treated with Pt before the SEM tests to make them conductive. High resolution images of catalysts were obtained via

the high-angle annular dark-field scanning transmission electron microscope (HAADF-STEM; FEI Titan Cubed Themis G2 300). X-ray diffraction (XRD; D8 Advance, Bruker, Germany) experiments were conducted at 40 kV and 40 mA with Cu K α radiation ($\lambda = 0.15418$ nm) to characterize the crystallography of catalysts. The catalysts were scanned at 4° min^{-1} from 15° to 85° at 0.01° intervals. An electron spectrometer (Thermo Fisher, ESCALAB 250Xi) with an Al K α ($h\nu = 1486.6$ eV) radiation source was employed to perform the X ray photoelectron spectroscopy (XPS), and the binding energy (BE) of carbon C1 s (284.8 eV) was used to calibrate the spectra.

4. Abiotic electrochemical tests

For chronoamperometry tests, a dual-chamber reactor with two cylindrical chambers (2 cm length each) and an anion exchange membrane (AMI-7001, Membrane International Inc., USA) was used as reported ². A three electrode system was used: the prepared air-cathodes were used as working electrodes, a saturated calomel electrode (SCE, 0.241 V vs. standard hydrogen electrode, SHE, Leici, China) placed adjacent to the air cathode was used as a reference electrode, and a platinum plate (99.99%, 1 cm²) was used as a counter electrode. A 50 mM phosphate buffer solution (PBS, containing 4.57 g L⁻¹ of Na₂HPO₄, 2.45 g L⁻¹ of NaH₂PO₄·H₂O, 0.31 g L⁻¹ of NH₄Cl, 0.13 g L⁻¹ of KCl) was used as electrolyte. Chronoamperometry tests were performed by an Autolab PGSTAT-204 potentiostat at 0.2, 0.1, 0, -0.1, -0.2, -0.3 and -0.4 V vs. SCE respectively, with each potential for 0.5 h.

To assess the ORR performance of the resultant catalysts, intensive electrochemical

tests were conducted via a rotating disk electrode (RDE) and a rotating ring-disk electrode (RRDE) setup (MSR rotator, PINE Instruments, USA) and an Autolab PGSTAT-128N potentiostat equipped with the Nova 1.10 software. It also adopted a three-electrode system: a 0.196 cm² rotating-disk (ring-disk) glassy-carbon electrode with catalysts served as the working electrode, a Pt electrode worked as the counter electrode and an Ag/AgCl (3 M KCl, +0.214 V vs. SHE) electrode was used as the reference electrode. The electrolytes adopted an O₂-saturated PBS (50 mM). To prepare a working electrode, 10 μL homogeneous ink consisting of catalysts, absolute ethyl alcohol and Nafion solution (5%) in the ratio of 5 mg: 95 μL: 5 μL was dripped onto the center of electrode and dried naturally. Both RDE and RRDE tests were performed at 1600 rpm with a sweep rate of 10 mV s⁻¹ at room temperature. For RRDE tests, the electron transfer number (n) and yield of hydrogen peroxide (% H₂O₂) were calculated as below:

$$n = 4 \times \frac{I_d}{I_d + I_r/N} \quad (2-1)$$

$$\%H_2O_2 = 200 \times \frac{I_r/N}{I_d + I_r/N} \quad (2-2)$$

where I_d and I_r represent the disk and ring current, respectively, and N=0.412 is the experimentally determined collection efficiency.

5. Scanning electrochemical microscopy experiments

Scanning electrochemical microscopy (SECM) experiments were conducted to study the microscopic electrochemical activities of resultant catalysts and Pt (the benchmark). A golden plate (d ~5 mm) encapsulated in epoxy resin (E-44 type) with catalysts functioned

as the working electrode. To prepare the working electrodes, the golden plate was divided into two parts, two kinds of homogeneous inks (5 μL each, the same with inks in RRDE tests in section 2.4) were dripped onto the two parts respectively (as showed in Figure S1a) and dried naturally. The scanning electrochemical microscopy (SECM) experiments were carried out on an AMETK setup (VersaSCAN) equipped with two electrochemical workstations (VersaSTAT 3 and VersaSTAT 3F). A four-electrode system was adopted, i.e. saturated calomel electrodes (SCE, 0.244 V vs. SHE) as the reference electrode, Pt as the counter electrode, a catalyst-coated golden plate as the working electrode and a probe (a 25 μm Pt microelectrode probe encapsulated in glass) as another working electrode. Mixture of 0.1 mol L^{-1} $\text{K}_3\text{Fe}(\text{CN})_6$ (as redox mediator) and 0.1 mol L^{-1} KCl (to promote the conductivity) was used as the electrolyte. The reactor was shown in Figure S1b. In the experiments, the probe was kept about 100 μm above the catalysts, which was confirmed by the approaching curve, and a 8000 μm \times 8000 μm square area was scanned. The potential on probe and catalysts were 0.7 V and -0.2 V (vs. SCE) respectively and the move steps in two directions were both 300 μm .

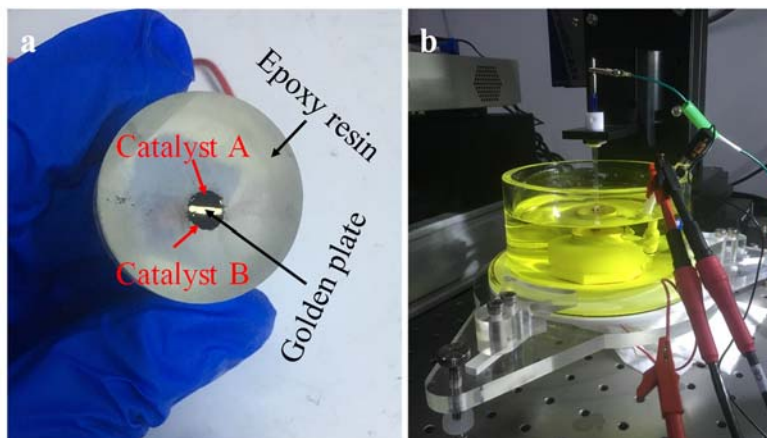


Figure S1. (a) The working electrode used in SECM experiment; (b) the reactor of SECM.

6. MFC tests

The MFC tests were conducted in single-chamber cubic-shaped MFC reactors as reported³. In a MFC reactor, a carbon brush served as the anode, and ~1 cm away from the anode is the prepared air-cathode with the diffusion layer facing the air. A saturated calomel electrode functioned as the reference electrode. The electrolytes adopted a synthetic wastewater which consisted of 1 g L⁻¹ of NaAc, 4.57 g L⁻¹ of Na₂HPO₄, 2.45 g L⁻¹ of NaH₂PO₄·H₂O, 0.31 g L⁻¹ of NH₄Cl, 0.13 g L⁻¹ of KCl, a mineral and a vitamin solution. By changing the external resistance from 5000 Ω to 10 Ω at a 20-min interval, the MFC voltages and anode potentials were recorded by a Keithley Series 2700 data acquisition system. Normalized current density (J) and power density (P) were calculated as follows to obtain the corresponding polarization curves and power density curves.

$$J = U/RA \text{ and } P = JU,$$

where U is the voltage, R is the external resistance and $A = 7 \text{ cm}^2$ is the projected area of the air cathode.

Additional Figures and Tables

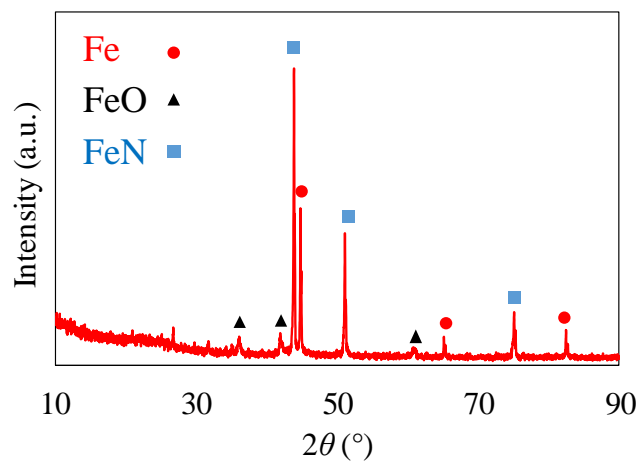


Figure S2. XRD patterns of Fe-clusters/NAC catalysts.

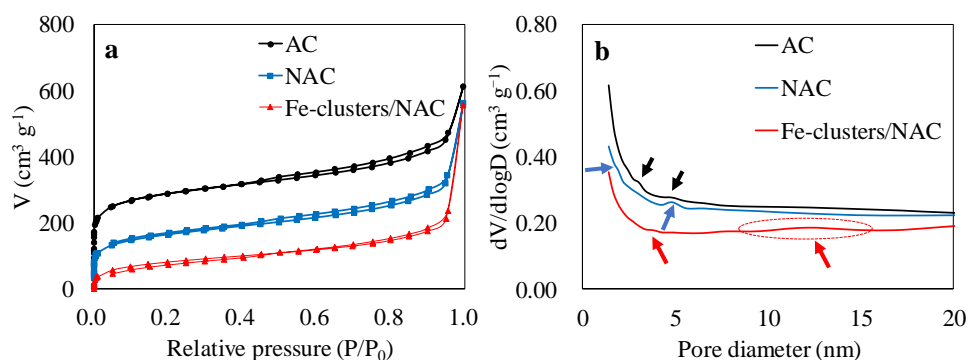


Figure S3. (a) N_2 adsorption-desorption plots of AC, NAC and Fe-clusters/NAC by BET method and (b) distribution of pores in AC, NAC and Fe-clusters/NAC catalysts by BJH method.

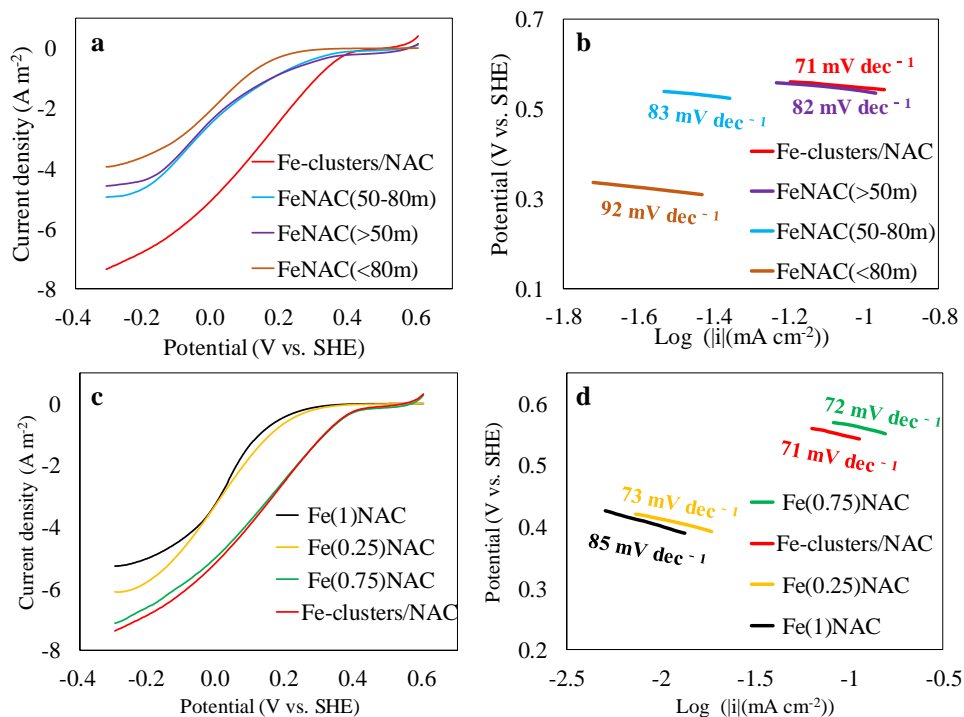


Figure S4. (a) (b) LSV curves and Tafel plots of Fe-clusters/NAC catalysts with different sizes and (c) (d) LSV curves and Tafel plots of Fe-clusters/NAC catalysts with different Fe contents based on RDE tests. Catalysts with sizes >50 meshes, 50-80 meshes, <80 meshes, and non-screening original catalysts, were marked as FeNAC(>50m), FeNAC(50-80m), FeNAC(<80m) and Fe-clusters/NAC, respectively. Catalysts with different Fe contents (weight ratios of AC and $\text{Fe}_2\text{O}_3 = 4:1, 2:1, 4:3$ and $1:1$), were marked as Fe(0.25)NAC, Fe-clusters/NAC, Fe(0.75)NAC and Fe(1)NAC, respectively.

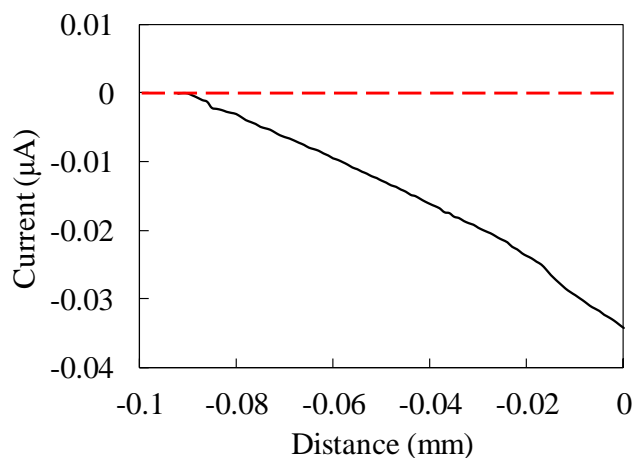


Figure S5. Approaching curve in SECM.

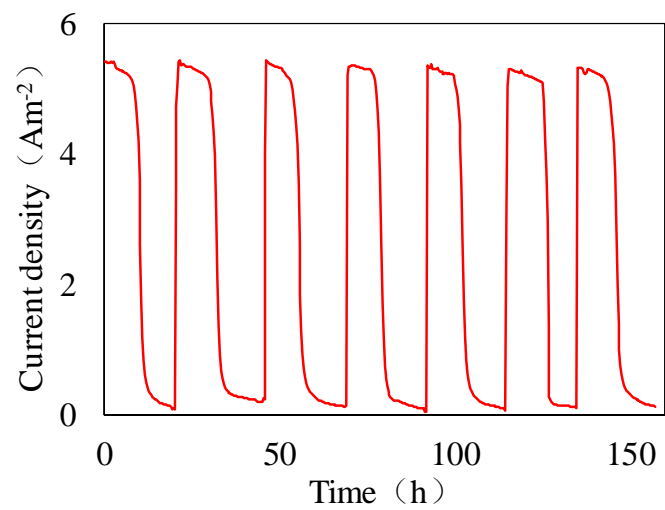


Figure S6. Current density changes with time of the MFC with Fe-clusters/NAC catalysts.

Table S1. Element contents of NAC and Fe-clusters/NAC based on XPS results

Samples	Element contents (at. %)			
	C	O	N	Fe
Fe-clusters/NAC	90.63	5.70	3.67	0.60
NAC	90.37	5.64	3.99	-

Table S2. Parameters of specific surface areas and pore structures of AC, NAC and Fe-clusters/NAC

Samples	Specific surface area ($\text{m}^2 \text{g}^{-1}$)	Mesoporous volume ($\text{cm}^3 \text{g}^{-1}$)	Average pore size (nm)
Fe-clusters/NAC	297.8	0.86	1.42
NAC	506.6	0.78	1.40
AC	965.8	0.78	1.36

Table S3. Comparison of the Fe/NC catalysts in MFCs reported in the last five years under the same/similar experimental conditions

MPD: the maximum power density of MFCs

MCD: the maximum current density of MFCs

NaAc: sodium acetate

Catalyst	MCD (A m ⁻²)	MPD (mW m ⁻²)	Anode Substrate	Electrolyte	Cathode size (cm ²)	Catalyst loading (mg cm ⁻²)	Reference
Fe-N-AC	11.4	2380	1 g L⁻¹ NaAc	50 mM PBS	7.0	2.9	This work
Fe-N-AC	~7.0	1092	1 g L ⁻¹ NaAc	100 mM PBS	7.0	15	Chem. Eng. J., 2019 , 361, 416-427 ⁴
Fe-N-AC	~6.2	2437	1 g L ⁻¹ NaAc	50 mM PBS	7.0	--	Bioresource Technol. 2016 , 206 ,285–289 ⁵
Fe-N-C/AC	~12.0 ~3.8	2600 800	1 g L ⁻¹ NaAc	50 mM PBS Domestic wastewater	7.0	27.0	ChemSusChem 2016 , 9, 2226 – 2232 ⁶
FePc/PID/CNTs	~4.5	799	1 g L ⁻¹ NaAc	PBS	7.0	0.5	Electrochim. Acta 2016 , 190, 388–395 ⁷
Fe-CNT(NH ₃)	4.3	742	1 g L ⁻¹ NaAc	PBS	7.0	0.5	Int. J. Hydrogen Energ. 2016 , 41, 19637 - 19644 ⁸
Fe-BP(NH ₃)	2.4	598					
Fe-N/G-90	~4.3	1210	NaAc	PBS	7.0	3.2	RSC Adv., 2018 , 8, 1203-1209 ⁹
Fe- N/G -60	~4.6	~981					
Fe-N/G -240	~4.0	~814					
Fe/N-HCN	~6.3	1300	1 g L ⁻¹ NaAc	50 mM PBS	--	2.0	J. Mater. Chem. A, 2017 , 5, 19343-19350 ¹⁰
Fe-NCB	~12.5	1850	20 mM Acetate	--	15.9	1.0	Electrochim. Acta, 2018 , 277, 127-135 ¹¹
Fe/C/Ns-900	~5.5	900	0.5 g L ⁻¹ NaAc	100 mM PBS	2.0	--	Appl. Surf. Sci. 2019 , 481, 1206–1212 ¹²
Fe/C/N-900	~4.0	660					
Fe-AAPyr	~7.5	1300	0.1 M NaAc	--	10.0	2.0	Energy, 2018 , 144, 1073-1079 ¹³
Fe-AAPyr	~3.5	780	--	50 mM PBS	4.0	5	ChemSusChem 2015 , 8, 828 – 834 ¹⁴
Fe-Mebendazole	~3.2	680					
Fe-AAPyr	~9.5	1670	1 g L ⁻¹ NaAc	50 mM PBS	2.9	2.1	Sci. Rep. 2015 , 5, 16596 ¹⁵
Fe-N-C	~16.5	1927	20 mM sodium lactate	100 mM PBS	6.0	2.0	Carbon, 2017 , 123, 481-491 ¹⁶

Fe-N-C	~5.2	1227	1 g L ⁻¹ NaAc	100 mM PBS	7.0	2.0	J. Power Sources 2016 , 315, 302-307 ¹⁷
Fe-PAA-90	~4.2	984	--	--	7.0	3.3	Catal. Commun., 2018 , 105,56-58 ¹⁸
Fe-N-SLG	~4.3	1210	1 g L ⁻¹ NaAc	50 mM PBS	7.0	5.7	J. Energy Chem., 2017 , 26, 1187-1195 ¹⁹
Fe-N-HCG	~4.5	~981					
Fe-N-HAG	~4.7	~988					
Fe ₃ O ₄ -N-C	~3.8	730	2 g L ⁻¹ NaAc	50 mM PBS	7.0	5.0	Biosens. Bioelectron., 2018 , 122, 113-120 ²⁰

Reference:

1. X. Zhang, H. Sun, P. Liang, X. Huang, X. Chen and B. E. Logan, *Biosens. Bioelectron.*, 2011, **30**, 267-271.
2. X. Guo, J. Jia, H. Dong, Q. Wang, T. Xu, B. Fu, R. Ran, P. Liang, X. Huang and X. Zhang, *J. Power Sources*, 2019, **414**, 444-452.
3. X. Zhang, W. He, W. Yang, J. Liu, Q. Wang, P. Liang, X. Huang and B. E. Logan, *Environ. Sci.: Water Res. Technol.*, 2016, **2**, 266-273.
4. Y. Liu, Y.S. Fan and Z.M. Liu, *Chem. Eng. J.*, 2019, **361**, 416-427.
5. Y. Pan, X. Mo, K. Li, L. Pu, D. Liu and T. Yang, *Bioresource Technol.*, 2016, **206**, 285-289.
6. W. Yang and B. E. Logan, *ChemSusChem*, 2016, **9**, 2226-2232.
7. M.T. Nguyen, B. Mecheri, A. Iannaci, A. D'Epifanio and S. Licoccia, *Electrochim. Acta*, 2016, **190**, 388-395.
8. A. Iannaci, B. Mecheri, A. D'Epifanio, M. J. Lázaro Elorri and S. Licoccia, *Int. J. Hydrogen Energ.*, 2016, **41**, 19637-19644.
9. D. Wang, Z. Ma, Y. E. Xie, Z. Man, Z. Na and H. Song, *Rsc Adv.*, 2018, **8**, 1203-1209.
10. L. Zhou, C. Yang, J. Wen, P. Fu, Y. Zhang, J. Sun, H. Wang and Y. Yuan, *J. Mater. Chem. A*, 2017, **5**, 19343-19350.
11. B. Erable, M. Oliot, R. Lacroix, A. Bergel, A. Serov, M. Kodali, C. Santoro and P. Atanassov, *Electrochim. Acta*, 2018, **277**, 127-135.
12. P. Ren, S. Ci, Y. Ding and Z. Wen, *Appl. Surf. Sci.*, 2019, **481**, 1206-1212.
13. I. Gajda, J. Greenman, C. Santoro, A. Serov, C. Melhuish, P. Atanassov and I. A. Ieropoulos, *Energy*, 2018, **144**, 1073-1079.
14. C. Santoro, A. Serov, C. W. Narvaez Villarrubia, S. Stariha, S. Babanova, A. J. Schuler, K. Artyushkova and P. Atanassov, *ChemSusChem*, 2015, **8**, 828-834.
15. C. Santoro, A. Serov, C. W. N. Villarrubia, S. Stariha, S. Babanova, K. Artyushkova, A. J. Schuler and P. Atanassov, *Sci. Rep.*, 2015, **5**, 16596(16591-16510).
16. X. Ma, Z. Lei, W. Feng, Y. Ye and C. Feng, *Carbon*, 2017, **123**, 481-491.
17. G. Lu, Y. Zhu, L. Lu, K. Xu, H. Wang, Y. Jin, Z. Jason Ren, Z. Liu and W. Zhang, *J. Power Sources*, 2016, **315**, 302-307.
18. D. Wang, Z. Ma, X. Meng and H. Song, *Catal. Commun.*, 2018, **105**, 56-58.
19. D. Wang, Z. Ma, Y. e. Xie and H. Song, *J. Energy Chem.*, 2017, **26**, 1187-1195.
20. H. Zhou, Y. Yang, S. You, B. Liu, N. Ren and D. Xing, *Biosens. Bioelectron.*, 2018, **122**, 113-120.